Received: 8 April 2020 | Revised: 15 July 2020 | Accepted: 22 July 2020

DOI: 10.1002/jbio.202000134

JOURNAL OF BIOPHOTONICS

FULL ARTICLE

Novel input polarisation independent endoscopic cross-polarised optical coherence tomography probe

Katharina Blessing[1,2*] | **Judith Schirmer**[1,2] | **Gargi Sharma**[3] | **Kanwarpal Singh**[1,2]

[1]Research Group Singh, Max Planck Institute for the Science of Light, Erlangen, Germany

[2]Department of Physics, Friedrich-Alexander Universität Erlangen-Nürnberg, Erlangen, Germany

[3]Guck Division, Max Planck Institute for the Science of Light, Erlangen, Germany

***Correspondence**
Katharina Blessing, Research Group Singh, Max Planck, Institute for the Science of Light, Staudtstraße 2, Erlangen 91058, Germany.
Email: katharina.blessing@mpl.mpg.de

Abstract

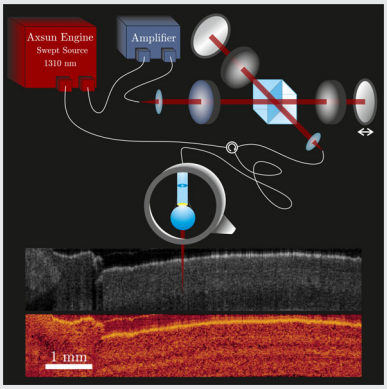

Lead by the original idea to perform non-invasive optical biopsies of various tissues, optical coherence tomography found numerous medical applications within the last two decades. The interference based imaging technique opens the possibility to visualise subcellular morphology up to an imaging depth of 3 mm and up to micron level axial and lateral resolution. The birefringence properties of the tissue are visualised with enhanced contrast using polarisation sensitive or cross-polarised optical coherence tomography (OCT) techniques. Although, it requires strict control over the polarisation states, resulting in several polarisation controlling elements. In this work, we propose a novel input-polarisation independent endoscopic system based on cross-polarised OCT. We tested the feasibility of our approach by measuring the polarisation change from a quarter-wave plate for different rotational angles. Further performance tests reveal a lateral resolution of 30 μm and a sensitivity of 103 dB. Images of the human nail bed and cow muscle tissue demonstrate the potential of the system to measure structural and birefringence properties of the tissue endoscopically.

KEYWORDS

endoscopy, medical imaging, optical biopsy, optical coherence tomography, polarisation sensitive methods

1 | INTRODUCTION

The early and specific detection of diseased tissue areas is crucial for successful therapy. During the last decades, endoscopy became a prominent diagnostic instrument for the detection of these areas, most commonly used in gastroenterology.[1] However, first structural changes often appear in deeper tissue layers and are hidden for

standard endoscopic imaging. Therefore, endoscopic optical coherence tomography (OCT) is known as a powerful tool to image tissue in its native state.[2] With its imaging depth of up to 3 mm, it opens the possibility to reveal diseased areas before they become prominent on the surface. Besides the two-dimensional, a three-dimensional representation of the tissue is feasible with OCT.[3] Though it is a relatively new approach, it found application in various medical fields. Besides for imaging the gastrointestinal tract,[4, 5] it is used to image coronary arteries,[6] to detect pulmonary lesions,[7, 8] to map lymph nodes in case of breast cancer,[9] to sense intraocular distances in ophthalmology[10] and for diagnostics in the field of onco-urology.[11] In recent years, several reviews on biomedical applications of improved OCT technology have been published.[12–15]

OCT is known as the optical equivalent to ultrasound imaging, that is it measures the echo of a signal coming from a light source reflecting from a sample. Since light travels too fast to detect the scattered signal directly, the acquisition is performed by detecting its interference pattern with a reference signal. Therefore, the first approaches were based on Michelson or Mach-Zehnder interferometers.[2] In this case, the changes in the interference pattern while changing the optical path difference between reference and sample arm are detected. Since constant detection through a defined interval is required to perform an A-scan, the imaging speed is limited to the time it takes to change the optical path difference physically. To accelerate the image acquisition to video-rate, the interference pattern can be measured while changing the frequency of the illumination either by applying a spectrometer or by sweeping through different wavelength within a specific interval. Data analysis, in this case, is performed in Fourier-domain instead of in real-space.[16]

Spectrometer based methods are more common in the clinical praxis. However, state-of-the-art swept-source based systems provide a higher scanning speed, in the case of an Axsun engine up to 200 kHz.[17] Furthermore, the narrow line width of the swept-source allows a higher spectral resolution than in the other systems. Thus, they provide extended scanning depth conjoined with increased sensitivity.[17] Perceiving these advantages in this paper, we present an expansion of a commercially available swept-source system, which enables to retrieve the birefringence properties of the sample.

As an interferometric method, OCT allows to retrieve the phase information of the reflected light from the sample, which in turn can be used to map the birefringence properties. To correctly retrieve this information, the polarisation state of the light source has to be controlled over the entire optical pathway. Following this condition, polarisation sensitive OCT (psOCT) devices have been reported. Many of them can display the full polarisation state of the light reflected by the sample that is give access to the full set of Stokes vectors. De Boer et al[18] and Baumann et al[19] published recent reviews discussing the advancement in this area.

However, a full control of the phase within the optical pathway is difficult to achieve with the random phase changes light experiences when it travels through a bent or stretched imaging fibre.[18] Thus, constructing endoscopic devices with a flexible probe provokes challenges, but the flexibility of the probes is crucial in clinical praxis. Nevertheless, probe-based psOCT systems have been reported and were successfully applied to image for example coronary arteries[20, 21] and to examine the condition of different parts of the lung.[22–24]

Nonetheless, under various circumstances, it is unnecessary to reconstruct the polarisation state entirely. Even though diattenuation seems to be negligible in tissue, it might cause ambiguities for interpreting the results due to birefringence only.[18] Depolarisation, for instance, helps to visualise melanin granules in pigmented tissue. Moreover, fibrous tissue like muscle, nerve fibre tissue and other tissues that contain collagen are mainly characterised by their birefringence properties.[25] Birefringence, in these cases, causes a depolarisation of the light reflected from the sample. Therefore, instead of allocating the entire polarisation state, devices only revealing the depolarisation light experiences while passing through the sample are satisfactory in many cases. Thus, another class of psOCT methods is introduced, the so-called cross-polarised OCT (cpOCT).

Image analysis in cpOCT requires two images, each illuminated with orthogonal polarised light.[26] The acquisition has been realised either sequentially[27] or simultaneously using depth encoding.[25, 28] Like for regular OCT and psOCT, time-domain, as well as frequency-domain approaches have been reported for cpOCT. Working in the frequency-domain and in case of depth encoded simultaneous acquisition; the illumination light signal is split into two orthogonal components. The image generated by light of the same polarisation as the input polarisation is defined as co-polarised (co), and the one generated by states orthogonal to the input polarisation is called cross-polarised (cross) image. For samples imaged with cpOCT systems, the intensity pattern of co- and cross-image differ from each other due to the combined effect of the orientation of the optical axis (with respect to the polarisation of the illuminating light) and light scattering. This difference was first reported by Schmitt and Xiang[29] for OCT systems. To quantify it, they suggest calculating the linear depolarisation ratio δ by determining the intensity ratio of cross- and co-image.

Despite the relatively low requirement for the control of the polarisation state, many of the reported systems still use several optical components, which are carefully aligned with respect to each other and depending on the polarisation-state of the light source. We recently developed a swept-source cpOCT system, which works for any input light polarisation and at the same time applying only one quarter-wave plate (QWP).[25] However, the polarisation state of the light source still has to be fixed before the data acquisition. During medical procedure, it might be unavoidable not to touch and move the system. Furthermore, physicians generally ask for a portable solution with little effort in prior adjustment. In this paper, we present a solution based on the swept-source engine, which delivers stable image quality, independent of fluctuations of the polarisation of the light source during the measurement. Thus, it does not need any prior alignment.

Several studies show the clinical relevance of cpOCT and a swept-source based system providing cpOCT, which was used for dental studies, is commercially available.[30] However, the probe of the system is rigid, and it does not give access to the co-polarised images. An ex-vivo study published last year defined visual assessment criteria to distinguish between tumorous and non-tumorous tissue intraoperatively with cpOCT in brain tumour imaging.[31] Another ex-vivo study shows its ability to distinguish fibrotic myocardium from normal or ablated myocardium in cardial imaging.[28] Particularly, these studies prove the necessity of endoscopic solutions with thin and flexible probes.

Single-mode fibres (SMF) provide the most straightforward option to serve as an imaging fibre in endoscopic OCT. Nevertheless, light travelling through a SMF might undergo unpredictable phase perturbations. Even in regular endoscopic OCT, these randomly occurring changes in the phase of the illumination or the length of the fibre decrease the image quality due to dispersion mismatches and systematically induced differences in length between reference and sample arm.[32] Common-path probes (CPP) help to overcome this problem.[33] These probes guarantee the balance of both, the dispersion and the phase, by detecting the interference pattern directly from the tip of the probe, that is reference and sample signal travel the same path, which experiences similar changes during the acquisition. We recently demonstrated a CPP design of a monolithic mirror-based CPP, which allows independent adjustment of working distance and reference power.[34, 35]

Targeting an endoscopic system with the ability to perform cpOCT, constructing the probe relying on an SMF as imaging fibre is an option also in this case. A closer look at the character of the polarisation changes light suffers during travelling through an SMF shows that its orthogonality is conserved and not affected by fibre movements. Gelikonov et al briefly discussed that, when presenting an entirely fibre based cpOCT system based on a Michelson interferometer.[26] Furthermore, in a later publication, they showed the value of CPP to construct systems with thin and flexible probes.[36] Nonetheless, they present a spectrometer-based system. Their approach addresses the problem caused by the wavelength dependency of polarisation, which leads to an instability of the illumination power in co- and cross-channel with a complex extension to the system for the active maintenance of the circular polarisation.

We present an approach, which impresses by its simplicity. Just by introducing a depolariser, we achieved an input polarisation independent cpOCT system. Here, we prove the efficiency of this simple solution, which makes the system not only insensitive to polarisation changes during the data acquisition, but also it minimises the necessity of prior adjustment. Applying a swept-source as the illumination source, we take advantage of its abilities concerning scanning depth and sensitivity. The monolithic mirror-based CPP allows to adapt the system to various requirements regarding the working distance.

2 | SYSTEM DESCRIPTION

Center of the system, schematically illustrated in Figure 1, is a swept-source OCT system supplied by Axsun (Axsun Technologies, North Billerica, Massachusetts). It works with a central wavelength of 1310 nm and a scan range of 140 nm at a sweeping rate of 100 kHz. The output power of the source is 24 mW. Additional to the illumination unit, the system comes with components for data acquisition and processing. Two photodiodes enabling balanced detection are coupled to a data acquisition card, a digitiser and a field-programmable gate array. As we are using the common path approach for our device, we use only one of the photodiodes.

To realise cpOCT, we build a free-space module. In the first step, light coming from the source is collimated by a fibre collimator delivered by Oz optics (HPUCO-13A-1300/1550-S-6.2AS, AMS Technologies AG)(C1). By a cubic polarising beam splitter (PBS-104, Thorlabs, Inc.) (PBS), the beam is divided into two linear polarised beams, which are orthogonal to each other. These beams are reflected by mirrors. One of the mirrors is mounted on a translational stage. This allows adjusting the distance between co and cross image during the data acquisition. The light reflected from the mirrors passes through the PBS again. We positioned achromatic QWP (AQWP10M-1600, Thorlabs, Inc.) in the paths between PBS and mirrors such that the reflected lights from the two mirrors are coupled into a

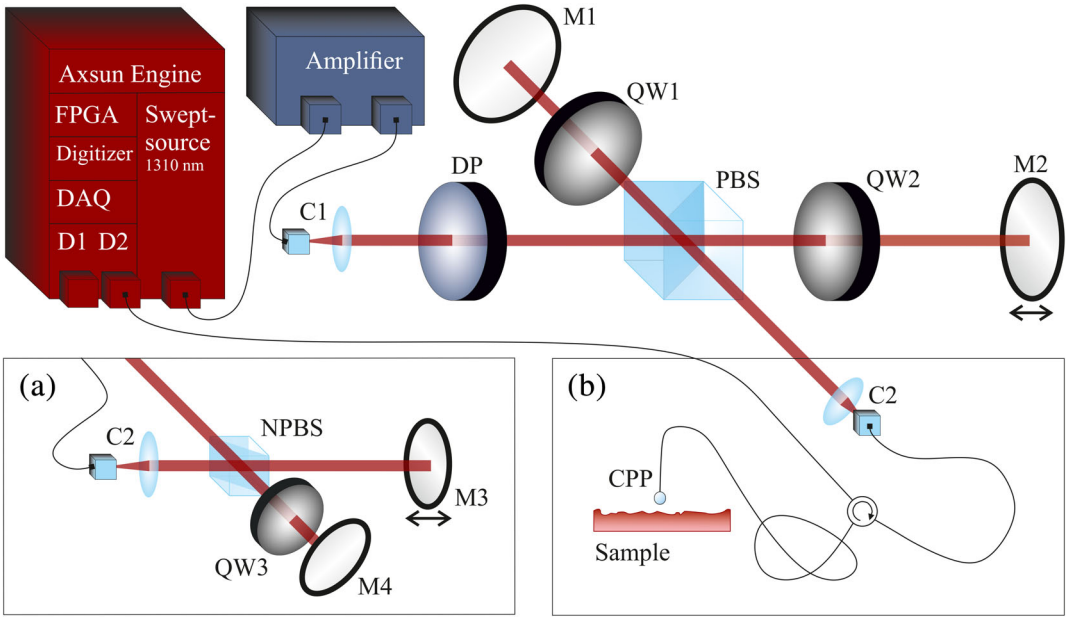

FIGURE 1 Scheme of the cross-polarised OCT system: The Axsun engine with swept-source, photodiodes (D1, D2), data acquisition card (DAQ), digitiser and field programmable gate array (FPGA), and the cross-polarised system with collimators (C1, C2), depolariser (DP), polarising beam splitter (PBS), quarter-wave plates (QW1, QW2) and the mirrors (M1, M2). A) shows the endoscopic probe (CPP), B) the experimental setup to characterise the birefringence properties of QW3 using a bench-top OCT system with a non-polarising beam splitter and mirrors (M3, M4). CPP, common-path probes; OCT, optical coherence tomography

broadband circulator (CIR-1310-50-APC, Thorlabs, Inc.) by another collimator (C2). The second output of the circulator is connected to the CPP and the third to one of the photodiodes of the Axsun engine.

CpOCT requires strictly orthogonal polarised light of the same illumination power in each channel. However, the swept-source provides elliptically polarised light, which leads to unequally distributed illumination power in the orthogonal channels after passing the PBS. To avoid this, a polarisation controller could be put at the output fibre of the light source to adjust the polarisation-state before each measurement and get circularly polarised light. The main disadvantage of this method is that the output fibre has to be fixed and should not be moved anymore, because even small shifts of this fibre change the polarisation state of the illumination and the system has to be realigned.

Aiming a system, which is insensitive to fibre movements of the output fibre as well as of the probe, we tested an alternative method. It is well known, that unpolarised light splits in two linearly polarised beams of equal power and orthogonal polarisation after passing through a PBS. Thus, we decided to depolarise the input illumination by a quartz wedge achromatic depolariser (DPU-25-C, Thorlabs, Inc.) (DP) positioned directly behind C1. This DP introduces a linear phase delay between orthogonal components along the beam wavefront. Thus, the beam after the depolariser is composed of a light signal, which has different polarisation directions at different locations within the beam. When such a signal is split into orthogonal components using a PBS, it splits into components of equal intensity. Furthermore, the two orthogonal components are still coherent as the phase delay between them is in the order of a few wavelengths. Thus, the phase delay introduces by the depolariser in our system is much less than the coherence length of our laser, which is 20 mm. Since the DP causes a small angle between the orthogonal states of the light source, direct coupling of light coming from the DP into an SMF is not recommended. However, the two mirrors allow us to compensate for the angular deviation and to couple the light into the CPP.

Although, the free-space module has a disadvantage: The power losses introduced by each component sum up in such a way that the sample illumination is not sufficient for a successful data acquisition any more. Without depolariser, we could couple 14.52 mW optical power to the fibre core using the collimator C2 (Figure 1) out of 18.24 mW laser power measured in front of the collimator C2, that is 80% of the signal was coupled into the fibre. Whereas, after putting the depolariser, the overall signal intensity before the second collimator (C2) drops to 16.02 mW. Out of it, we coupled 9.64 mW, which results in an efficiency of 60%. The increased coupling losses for the orthogonal light components at the collimator C2 can be attributed to the deviation of the wavefront from the Gaussian shape.

The signal coupled to the probe is cut in half by the reference mirror in the probe. There are additional losses (approximately 30%) from the circulator in the system after the collimator C2. To compensate for the losses, we amplified the output power of the swept-source with a signal amplifier (Series CLD1000, Model CLD1015, Thorlabs, Inc.).

As mentioned above, data acquisition is directly performed by the Axsun engine. Furthermore, the engine performs the data processing. As an output, it exports the intensity pattern in JPEG format. Therefore, the digitised signal is processed on the field programmable gate array, which includes Hamming windowing of the spectrum, background subtraction and Fourier transformation before the image conversion. The images are transferred to a workstation for further processing via ethernet cable.

For our system, each JPEG-image contains three depth encoded representations of the same tissue area. The three images of the tissue are a result of the possible combination of the optical path difference (OPD) between the reference signal reflected from the reference mirror and the sample signal reflected from the tissue. If the initial OPD between the two orthogonal states generated from mirror M1 and M2 is Δd_1 and the distance of the sample from the reference mirror is Δd_2, then two cross-polarised images will be generated at $\Delta d_2 - \Delta d_1$ and $\Delta d_2 + \Delta d_1$, and one co-polarised image will be generated at Δd_2. Thus, the central intensity distribution is the co-image I_{co}, while the intensity distribution of the cross-image I_{cross} is given by the superposition of the other two. To extract the data, we first separated the images from each other. Afterwards, we used the following formula to evaluate the cross-image I_{cross} out of the two outer distributions.

$$I_{\text{cross}} = \sqrt{I_{\text{cross1}}^2 + I_{\text{cross2}}^2}. \tag{1}$$

where I_{cross1} denotes the intensity distribution of the upper and I_{cross2} the intensity distribution of the lower image.

Out of the co- I_{co} and the cross- I_{cross} image, we calculated the depolarization ratio δ and the standard representation of an OCT signal given by the reflectivity R of the sample.[29] Notably, no further correction of the images is required.

$$\delta = \frac{I_{\text{cross}}}{I_{\text{co}}}. \tag{2}$$

$$R = \sqrt{I_{\text{cross}}^2 + I_{\text{co}}^2}. \tag{3}$$

We determined the sensitivity of the system with a method established previously.[37] Therefore, we identified the maximal possible power coupling back into the probe after the signal is reflected from a sample mirror placed in front of the probe. By tilting the mirror, we reduced the sample signal by a known value. Afterwards, we computed the signal to noise ratio of the resulting interference pattern in the Fourier-domain and added the value of sample signal reduction. To examine the resolution of the system, we imaged a variable line grating from Thorlabs (R1L3S6P, Thorlabs, Inc.) with our probe.

Additionally, we measured the changes of intensity in co- and cross-image of light by passing through a QWP at different illumination angles. Afterwards, we calculated δ to prove that our proposed method reveals the birefringence properties of a sample. For the cpOCT system characterisation, as we are using the common path probe, it was not possible to place the QWP in the sample arm. Therefore, we modified the experimental set-up, as shown in Figure 1B. After the separation of reference and sample arm by a 50:50 non-polarising beam-splitter (NPBS) (Thorlabs Inc.), the QWP was positioned in the sample arm and a mirror was put at the sample position. By rotating the QWP, we captured one image every four degrees, analysed the data in the described manner and plotted the depolarisation ratio δ over the acquisition angle.

After characterising the system, we imaged the nail bed of a human volunteer and some cow muscle tissue provided by a local butcher shop. The maximal depth range of our system is 5 mm, which is further reduced by multiple noise lines appearing from the interference between different optical components in the system The tissue was cut in thin slices in order to avoid overlapping of co- and cross-images. We show co- and cross-image, as well as the image arising from standard OCT (standard), characterised by the reflectivity, and the one from the depolarisation ratio δ.

Furthermore, we measured the input polarisation dependence of the light source by placing a polarisation controller at the output fibre of the light source before the light passes the collimator C1. With a power meter (PM400, Thorlabs, Inc.), we monitored the intensity fluctuation in one of the illumination channels (from mirror M1) after blocking the illumination coming from the other illumination channel (from mirror M2) while moving the arms of the polarisation controller. We did these measurements using the system in its reported state and after removing the DP.

Likewise, we show the influence of the intensity fluctuations referred to the image quality firstly by imaging plain paper while moving the polarisation controller at the output fibre of the light source with the complete system (with DP) and after removing the DP. We repeated these measurements with cow muscle tissue.

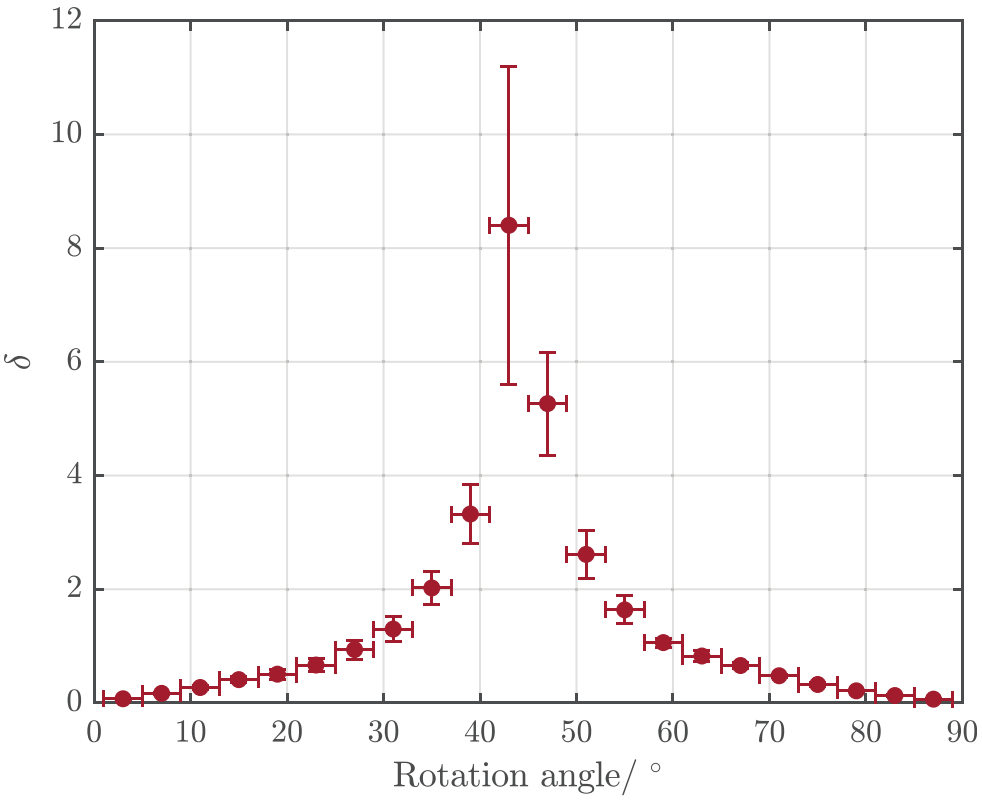

FIGURE 2 System Validation: Measurement of the depolarisation ratio δ introduced by a (QWP), which is placed in the sample arm of the system and the illumination reflected by a mirror. QWP, quarter-wave plates

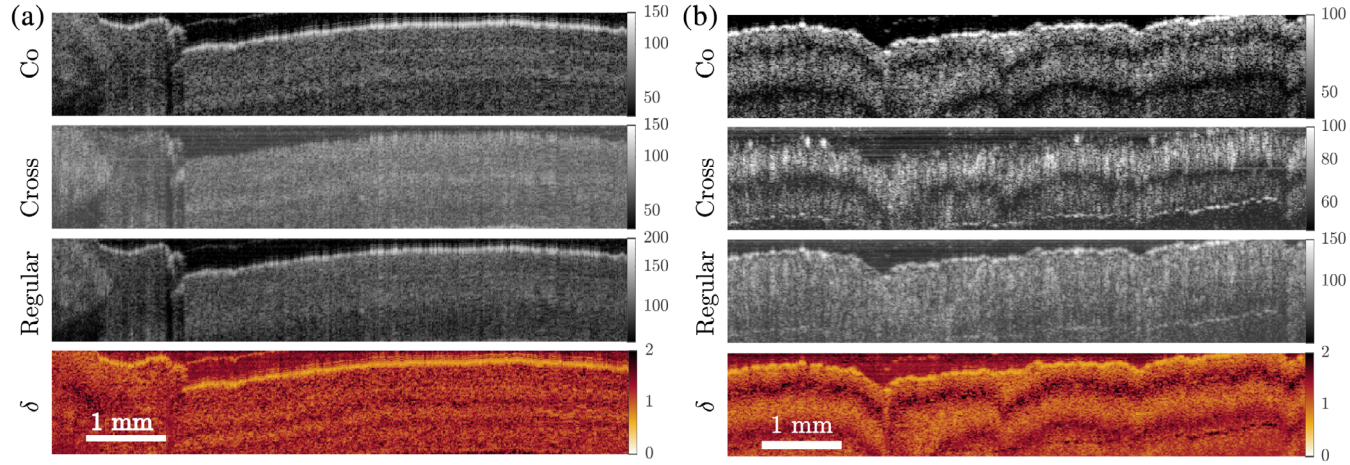

FIGURE 3 Results of the tissue imaging: Separated co- and cross-images and the reflectivity of the sample denoted with standard. The relative intensity values of the upper three images are encoded in the greyscale. The colorbar of the last image displays the depolarisation ratio δ

3 | RESULTS

Our measurements revealed that the endoscopic approach described in Section 2 provides images with a lateral resolution of 30 μm (see supplementary figure). With a sample illumination power of 13.4 mW we obtained a sensitivity of 103 dB. The graph in Figure 2 displays the regular angular dependency of the depolarisation ratio δ we expect from light passing through a QWP. Thus, it proves that differences between the intensity distributions are induced by the birefringence properties of the sample.

Figure 3 displays the results of the tissue imaging. Although the images show phase accumulation effects in form of periodic band like patterns, the layered intensity pattern introduced by the tissue birefringence can be recognised in both sets of images, nail bed, and cow muscle tissue. Notably, the standard OCT images hides the

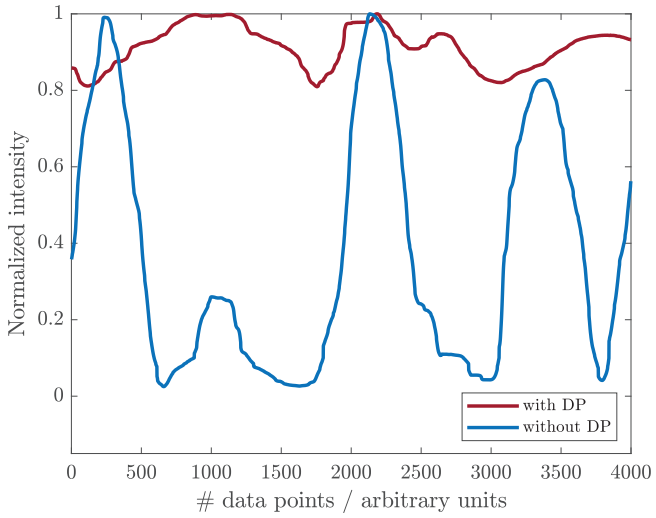

FIGURE 4 Intensity fluctuations the sample illumination experiences with and without the DP in the beam-path directly behind the illumination output: For the measurement the intensity fluctuations were monitored while moving the output fibre of the illumination. DP, depolariser

birefringence details of the tissue, which makes the necessity of cpOCT for further structural analysis evident. Though it is marginal, in both datasets, (a) and (b), a thin reflection from the lens surface of the probe appears above the tissue. More careful engineering of the probe could help to avoid that.

For measuring the input polarisation dependence, we monitored the relative change of the power after moving the arm of the polarisation controller with and without DP. In Figure 4, we plot the intensity fluctuations in the sample illumination over the consecutively taken data points while slowly moving the arms of the polarisation controller forwards and backwards. For the normalisation, the maximal intensity is taken. These measurements show that the power fluctuations are significantly higher when we remove the DP from the system.

Figure 5 highlights the relevance of the DP for the image quality. After showing the intensity fluctuations in one of the orthogonal channel graphically, see Figure 4, we imaged paper and cow muscle tissue while

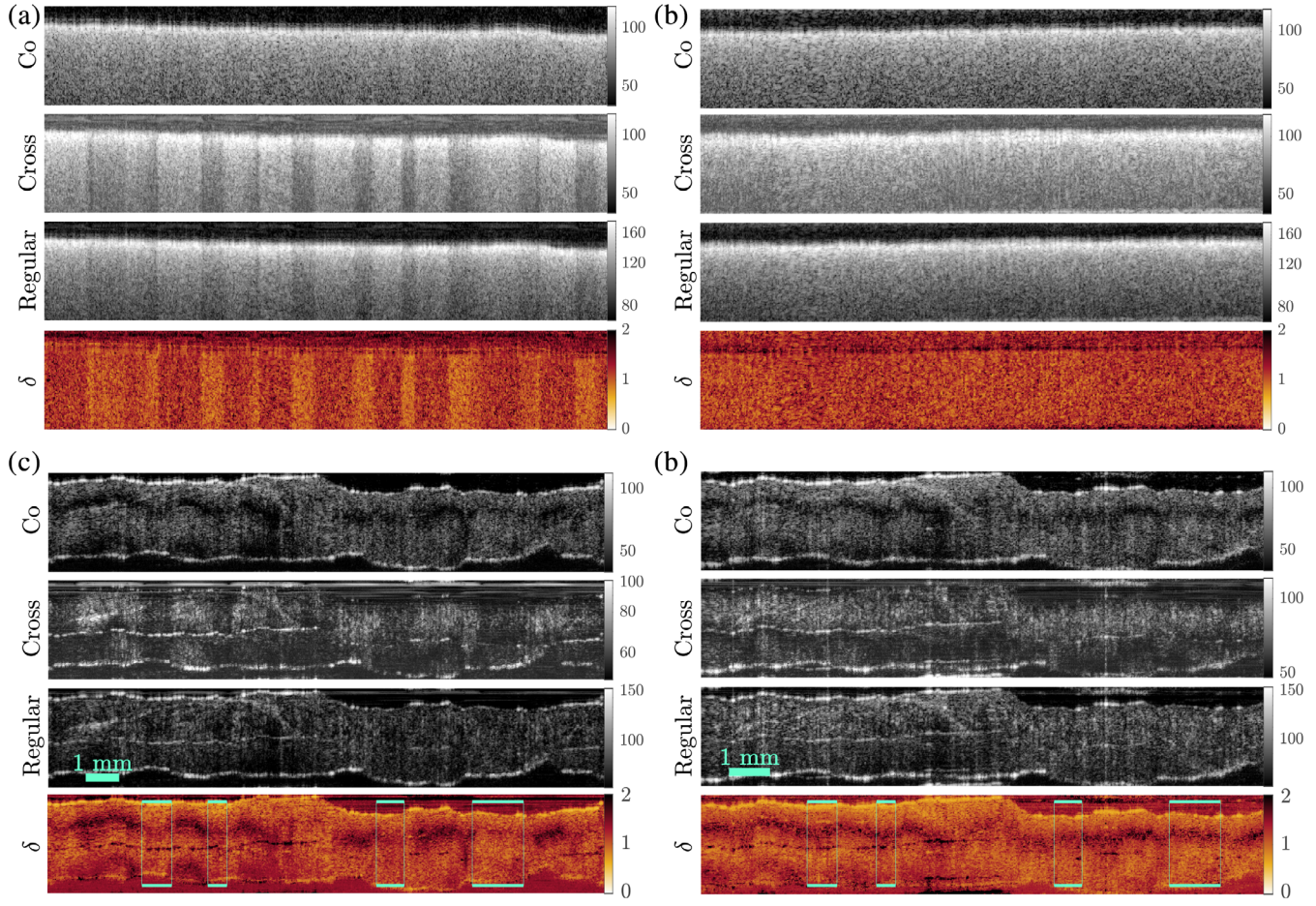

FIGURE 5 Impact of the intensity fluctuation for actual sample imaging: For all images, the output fibre was moved randomly to introduce phase fluctuations of the illumination. Like in Figure 3 the co, the cross and the regular representation are shown, as well as the depolarisation ratio δ. A and B show paper firstly imaged without DP (a) and compared with the sample imaged after positioning the DP (b). (c) shows cow muscle tissue again imaged with the system lacking the DP while (d) depicts the same sample acquired with the complete system

moving the polarisation controller. Though paper is a highly scattering material without any birefringence, the images without the DP, Figure 5A, depict stripes in the orthogonal channel which arise only due to the fluctuations of the illumination power among the orthogonal components of the illumination signal. Such image artefacts lead to a misinterpretation of the sample structure. After putting the DP, these stripes nearly vanish as demonstrated in Figure 5B, which prompts that the fluctuations arising from sudden polarisation changes are sufficiently reduced.

The importance of a more or less constant illumination power in both channels is even more apparent if the birefringence properties of a sample are of interest for the interpretation of the state of a sample, for example in tissue. In Figure 5C,D we show the images of cow muscle tissue. The artefacts because of unequal power in the orthogonal channels are most clearly pronounced in the last image of Figure 5C, which illustrateδ. The areas where the differences between c and d appear are featured with turquoise boxes. Within these areas indicated by boxes, in Figure 5 c alternating intensity bands, which result from tissue birefringence nearly vanishes. At the same time, such artefacts are not visible in images obtained with DP in the system (5d). Thus, if the illumination power in the orthogonal channel drops too low, the representation showing δ will assimilate to the regular OCT representation.

4 | CONCLUSION

In summary, we present a novel cpOCT approach. Based on a commercially available swept-source engine, it provides a sensitivity of 103 dB at a sample power of 13.4 mW. Although it is an endoscopic system, its performance is comparable to the previously reported bench-top cpOCT system[25] in terms of sensitivity and resolution. The measurements with a QWP demonstrate that the system reliably displays the birefringence properties of a sample.

The tissue images reveal additional details, particularly the birefringence properties of the sample, which cannot be displayed by regular OCT devices. Reader should note here that the phase difference between the orthogonal channels measured using cpOCT is an accumulated phase difference along the beam path inside the tissue and not the local phase difference. The accumulated phase difference is a combined result of the retardance introduced by the sample birefringence and the phase difference introduced by the optical axis orientation. Unlike psOCT imaging where the retardance and optical axis orientation can be determined separately, in cpOCT, a combined effect of both is measured. Therefore, the local retardance cannot be determined in cpOCT. This is not the limitation of our method, but in general, a limitation of the cpOCT technique compared to the psOCT.

A technical challenge of our current system is that we still have to measure thin tissue because of the limited depth range of 5 mm. For future applications when imaging inside the body, the free-space module has to be combined with an engine, which provides a depth range of at least three times the required depth range for conventional endoscopic OCT imaging in the region of interest. Considering a maximal penetration depth of 3 mm, an engine providing a depth range of 10 mm combined with the reported free space module would solve the problem for bench-top systems. For endoscopic systems, the requirements are even higher since the probe has to accommodate to the different working distance requirements, for example due to natural variance in diameter of the luminal structures.

Nevertheless, the thin and flexible probe in combination with a different engine offers new possibilities, for example in the circumferential imaging of coronary arteries if the probe is angle polished to make it side viewing and connected to a rotary junction. Several suggestions to realise such kind of changes have been made.[33] The working distance of the CPP can be adapted to the requirements.

Remarkably, we could demonstrate that the DP sufficiently reduces the fluctuations of the illumination power for imaging under clinical conditions where movements of the device are sometimes unavoidable. This is especially highlighted in Figure 5.

In conclusion, supplementary figure we believe that the concept presented here of a simple endoscopic cpOCT system can be transferred into a useful diagnostic tool for intraoperative imaging. Fibrous material and tumorous tissue, for example, can be characterised by changes in the birefringence properties. Since the image quality is barely affected by fluctuations of the polarisation of the light source, it can be easily converted into a portable system with little efforts of prior adjustment. Moreover, during a medical procedure, it promises constant image quality even if the system is misaligned or it has to be repositioned. Thus, we hope that this approach would be a significant step towards non-invasive optical biopsies.

ACKNOWLEDGMENTS

Open access funding enabled and organized by Projekt DEAL.

AUTHOR BIOGRAPHIES

Please see Supporting Information online.

CONFLICTS OF INTEREST

The authors declare no potential conflict of interests.

DATA AVAILABILITY STATEMENT

Data available on request from the authors.

ORCID

Katharina Blessing https://orcid.org/0000-0002-2395-3440
Kanwarpal Singh https://orcid.org/0000-0002-6884-8089

REFERENCES

[1] M. N. R. Kiesslich, P. R. Galle, M. F. Neurath, *Atlas of Endomicroscopy*, Springer Medizin Verlag Heidelberg, Berlin: Springer Verlag, Berlin, **2008**.
[2] D. Huang, E. A. Swanson, C. P. Lin, J. S. Schuman, W. G. Stinson, W. Chang, M. R. Hee, T. Flotte, K. Gregory, C. A. Puliafito, *Science.* **1991**, *254*, 1178.
[3] J. G. Fujimoto, W. Drexler, *Optical Coherence Tomography Technology and Applications*, Springer Reference **2015**.
[4] A. M. Sergeev, V. M. Gelikonov, G. V. Gelikonov, F. I. Feldchtein, R. V. Kuranov, N. D. Gladkova, N. M. Shakhova, L. B. Snopova, A. V. Shakhov, I. A. Kuznetzova, A. N. Denisenko, V. V. Pochinko, Y. P. Chumakov, O. S. Streltzova, *Opt. Express* **1997**, *1*, 432.
[5] B. E. Bouma, G. J. Tearney, C. C. Compton, N. S. Nishioka, *Gastrointest. Endosc.* **2000**, *51*, 467.
[6] H. G. Bezerra, M. A. Costa, G. Guagliumi, A. M. Rollins, D. I. Simon, *J. Am. Coll. Cardiol. Intv.* **2009**, *2*, 1035.
[7] M. Tsuboi, A. Hayashi, N. Ikeda, H. Honda, Y. Kato, S. Ichinose, H. Kato, *Lung Cancer* **2005**, *49*, 387.
[8] S. Lam, B. Standish, C. Baldwin, A. McWilliams, J. leRiche, A. Gazdar, A. I. Vitkin, V. Yang, N. Ikeda, C. MacAulay, *Clin. Cancer Res.* **2008**, *14*, 2006.
[9] F. T. Nguyen, A. M. Zysk, E. J. Chaney, S. G. Adie, J. G. Kotynek, U. J. Oliphant, F. J. Bellafiore, K. M. Rowland, P. A. Johnson, S. A. Boppart, *IEEE Eng. Med. Biol. Mag.* **2010**, *29*, 63.
[10] A. F. Fercher, C. K. Hitzenberger, G. Kamp, S. Y. El-Zaiat, *Optics Commun.* **1995**, *117*, 43.
[11] S. Kharchenko, J. Adamowicz, M. Wojtkowski, T. Drewa, *Central European J Urol.* **2013**, *66*, 136.
[12] A. F. Fercher, W. Drexler, C. K. Hitzenberger, T. Lasser, *Rep. Prog. Phys.* **2003**, *66*, 239.
[13] A. M. Zysk, F. T. Nguyen, A. L. Oldenburg Daniel, L. Marks Stephen, A. Boppart M.D., *J. Biomed. Opt.* **2007**, 12, https://doi.org/10.1117/1.2793736.
[14] M. Adhi, J. S. Duker, *Curr. Opin. Ophthalmol.* **2013**, *24*, 213.
[15] H. F. Z. X. Shu, L. J. Beckmann, *J. Biomed. Opt.* **2017**, *22*.
[16] R. Leitgeb, C. K. Hitzenberger, A. F. Fercher, *Opt. Express* **2003**, *11*, 889.
[17] W. Drexler, M. Liu, A. Kumar, T. Kamali, A. Unterhuber, R. A. Leitgeb, *J. Biomed. Opt.* **2014**, *19*, 071412.
[18] J. F. de Boer, C. K. Hitzenberger, Y. Yasuno, *Biomed. Opt. Express* **2017**, *8*, 1838.
[19] B. Baumann, *Appl. Sci.* **2017**, *7*(5), 474.
[20] S. D. Giattina, B. K. Courtney, P. R. Herz, M. Harman, S. Shortkroff, D. L. Stamper, B. Liu, J. G. Fujimoto, M. E. Brezinski, *Int. J. Cardiol.* **2006**, *107*, 400.
[21] M. Villiger, B. Braaf, N. Lippok, K. Otsuka, S. K. Nadkarni, B. E. Bouma, *Optica* **2018**, *5*, 1329.
[22] J. Li, F. Feroldi, J. d. Lange, J. M. A. Daniels, K. GrÃijnberg, J. F. de Boer, *Opt. Express* **2015**, *23*, 3390.
[23] L. P. Hariri, M. Villiger, M. B. Applegate, M. Mino-Kenudson, E. J. Mark, B. E. Bouma, M. J. Suter, *Am. J. Respir. Crit. Care Med.* **2013**, *187*, 125.
[24] D. C. Adams, L. P. Hariri, A. J. Miller, Y. Wang, J. L. Cho, M. Villiger, J. A. Holz, M. V. Szabari, D. L. Hamilos, R. S. Harris, J. W. Griffith, B. E. Bouma, A. D. Luster, B. D. Medoff, M. J. Suter, *Sci. Transl. Med.* **2016**, *8*, 359ra131.
[25] G. Sharma, S. Sharma, K. Blessing, G. Hartl, M. Waldner, K. Singh, *J Opt.* **2020**, *22*, 045301.
[26] V. M. Gelikonov, G. V. Gelikonov, *Laser Phy Lett.* **2006**, *3*(9), 445.
[27] R. V. Kuranov, V. V. Sapozhnikova, I. V. Turchin, E. V. Zagainova, V. M. Gelikonov, V. A. Kamensky, L. B. Snopova, N. N. Prodanetz, *Opt. Express* **2002**, *10*, 707.
[28] X. Yao, Y. Gan, Y. Ling, C. C. Marboe, C. P. Hendon, *J. Biophotonics* **2018**, *11*, e201700204.
[29] J. M. Schmitt, S. H. Xiang, *Opt. Lett.* **1998**, *23*(13), 1060.
[30] P. Lenton, J. D. Rudney, A. Fok, R. S. Jones, *J Med Imaging* **2014**, *1*, 016001.
[31] K. S. Yashin, E. B. Kiseleva, E. V. Gubarkova, A. A. Moiseev, S. S. Kuznetsov, P. A. Shilyagin, G. V. Gelikonov, I. A. Medyanik, L. Y. Kravets, A. A. Potapov, E. V. Zagaynova, N. D. Gladkova, *Front. Oncol.* **2019**, *9*, 201.
[32] K. Singh, G. Sharma, G. J. Tearney, *J Opt.* **2018**, *20*, 025301.
[33] M. J. Gora, M. J. Suter, G. J. Tearney, X. Li, *Biomed. Opt. Express* **2017**, *8*(5), 2405.
[34] K. Singh, R. Reddy, G. Sharma, Y. Verma, J. A. Gardecki, G. Tearney, *Lasers Surg. Med.* **2018**, *50*, 230.
[35] K. Blessing, S. Sharma, A. Gumann, K. Singh, *Eng Res Express* **2019**, *1*, 025008.
[36] V. M. Gelikonov, V. N. Romashov, D. V. Shabanov, S. Y. Ksenofontov, D. A. Terpelov, P. A. Shilyagin, G. V. Gelikonov, I. A. Vitkin, *Radiophy Quantum Electron.* **2018**, *60*, 897.
[37] K. Singh, D. Yamada, G. Tearney, *Sovremennye Tehnol Med.* **2015**, *7*(1), 29.

SUPPORTING INFORMATION

Additional supporting information may be found online in the Supporting Information section at the end of this article.

How to cite this article: Blessing K, Schirmer J, Sharma G, Singh K. Novel input polarisation independent endoscopic cross-polarised optical coherence tomography probe. *J. Biophotonics*. 2020; e202000134. https://doi.org/10.1002/jbio.202000134